

**MODELLING OF INHOMOGENEOUS VERTICAL  
UNDERWATER OPTICAL WIRELESS  
COMMUNICATION LINKS**

**MUHAMMAD SAFIY BIN SABRIL**

**UNIVERSITI SAINS MALAYSIA**

**2023**

**MODELLING OF INHOMOGENEOUS VERTICAL  
UNDERWATER OPTICAL WIRELESS  
COMMUNICATION LINKS**

by

**MUHAMMAD SAFIY BIN SABRIL**

**Thesis submitted in fulfilment of the requirements  
for the degree of  
Master of Science**

**March 2023**

## ACKNOWLEDGEMENT

All gratitude is due to Allah S. W. T., the Lord of the Universe, for providing me with the strength, direction, and patience needed to accomplish my thesis. I am very thankful to my supervisor, Dr. Faezah Jasman, for her great supervision, useful assistance, patience, methodical way of thinking, beneficial talks, and ongoing support. I am glad for the chance to work under her guidance. I would like to thank my co-supervisor, Dr. Wan Hafiza Wan Hassan, for her insightful conversations, remarks, and assistance. I would like to thank Ministry of Higher Education Malaysia through Fundamental Research Grant Scheme (Project Code: FRGS/1/2019/TK04/USM/02/15) for providing graduate financial assistance. I would also want to thank everyone at the Institute of Nano Optoelectronics Research and Technology (INOR), Universiti Sains Malaysia. My heartfelt thanks and love to my parents, Rogayah Osman and Othman Awang, for their encouragement and support throughout the writing of my thesis. Last but not least, I want to thank my dear girlfriend Adilah for sharing ideas and encouraging me.

## TABLE OF CONTENTS

<b>ACKNOWLEDGEMENT</b> .....	<b>ii</b>
<b>TABLE OF CONTENTS</b> .....	<b>iii</b>
<b>LIST OF TABLES</b> .....	<b>vi</b>
<b>LIST OF FIGURES</b> .....	<b>vii</b>
<b>LIST OF SYMBOLS</b> .....	<b>x</b>
<b>LIST OF ABBREVIATIONS</b> .....	<b>xi</b>
<b>LIST OF APPENDICES</b> .....	<b>xii</b>
<b>ABSTRAK</b> .....	<b>xiii</b>
<b>ABSTRACT</b> .....	<b>xv</b>
<b>CHAPTER 1 INTRODUCTION</b> .....	<b>1</b>
1.1 Introduction .....	1
1.2 Problem statement and motivations .....	3
1.3 Objectives.....	5
1.4 Scope of research .....	6
1.5 Thesis outline .....	7
<b>CHAPTER 2 LITERATURE REVIEW</b> .....	<b>8</b>
2.1 Introduction .....	8
2.2 Overview on underwater wireless communication .....	8
2.3 Underwater optical wireless communication .....	10
2.4 Inherent optical properties.....	13
2.4.1 Absorption and scattering coefficients.....	15
2.4.2 Volume scattering function .....	16
2.5 Vertical link properties.....	17
2.5.1 Vertical distribution of chlorophyll-a.....	18
2.5.2 Depth dependent refractive index .....	18

2.6	Beer's law and radiative transfer equation.....	19
2.7	Homogeneous model.....	20
2.7.1	Initial preparations.....	21
2.7.2	Initial photon position .....	22
2.7.3	Photon path length.....	23
2.7.4	Photon weight.....	24
2.7.5	Photon scattering .....	25
2.7.6	Updating photon direction.....	25
2.7.7	Updating photon position .....	26
2.7.8	Reception.....	26
2.8	Recent work on channel modelling .....	26
2.8.1	Horizontal link.....	26
2.8.2	Vertical link.....	29
2.9	Summary .....	31
<b>CHAPTER 3 METHODOLOGY.....</b>		<b>33</b>
3.1	Introduction .....	33
3.2	Overall procedure .....	33
3.3	Overview of Monte Carlo technique .....	34
3.4	Inhomogeneous model .....	35
3.4.1	Medium structure: homogeneous and inhomogeneous models .....	36
3.4.2	Alteration on the photon path length.....	38
3.4.3	Alteration on the photon's new direction.....	38
3.4.4	Model II and Model III: Importing vertical profiles of chlorophyll concentration.....	40
3.5	Simulation parameters .....	43
3.6	Calculation of impulse and frequency responses .....	44
3.7	Optimum design for receiver parameters .....	46
3.8	Summary .....	47

<b>CHAPTER 4</b>	<b>RESULTS AND DISCUSSION.....</b>	<b>48</b>
4.1	Introduction .....	48
4.2	Path loss.....	48
4.3	Impulse response .....	53
4.4	Frequency response .....	58
4.5	The effect of receiver FOV .....	64
4.5.1	Path loss.....	65
4.5.2	Frequency response .....	68
4.6	The effect of receiver aperture .....	73
4.6.1	Path loss.....	73
4.6.2	Frequency response .....	76
4.7	The optimal design of receiver’s aperture and field-of-view (FOV) .....	81
4.8	Summary .....	84
<b>CHAPTER 5</b>	<b>CONCLUSION AND FUTURE RECOMMENDATIONS.....</b>	<b>86</b>
5.1	Conclusion.....	86
5.2	Recommendations for Future Research .....	87
<b>REFERENCES.....</b>		<b>89</b>
<b>APPENDICES</b>		
<b>LIST OF PUBLICATIONS</b>		

## LIST OF TABLES

	<b>Page</b>
Table 1.1	Description of UWC technologies from (Ali et al., 2020; Islam et al., 2022).....3
Table 2.1	List of works on channel modelling and characterization of horizontal link .....28
Table 3.1	Regression equation to estimate the chlorophyll concentration from (Kameda & Matsumura, 1998).....41
Table 3.2	Vertical depth profile of temperature, salinity and pressure of ocean water from (Castelão, 2017) .....43
Table 3.3	Attenuation coefficients of two water types in homogeneous and inhomogeneous medium from(Kameda & Matsumura, 1998) .....43
Table 3.4	Simulation parameters.....44
Table 4.1	RMS delay spread (s) of the collimated links for low and high chlorophyll concentration.....58
Table 4.2	RMS delay spread (s) of the diffused links for low and high chlorophyll concentration.....58
Table 4.3	The 3 dB bandwidth of the collimated links for low and high chlorophyll concentration.....64
Table 4.4	The 3 dB bandwidth of the diffused links for low and high chlorophyll concentration.....64
Table 4.5	Summary of the proposed optimum design .....84

## LIST OF FIGURES

	<b>Page</b>
Figure 1.1	The basic structure of an underwater wireless communication adapted from (Wang et al., 2021).....2
Figure 2.1	Illustration of underwater optical wireless communication..... 10
Figure 2.2	Absorption coefficient of pure seawater for different light wavelengths extracted from (Schirripa Spagnolo et al., 2020) ..... 12
Figure 2.3	Geometry used to define the inherent optical properties of water from (Mobley 1994)..... 13
Figure 2.4	Transmitter (Tx) and receiver (Rx) in a Cartesian coordinate system with the appropriate wavelength for the underwater environment..... 22
Figure 3.1	Flowchart of methodology ..... 34
Figure 3.2	Flowchart shows process for transmitting photon from transmitter to receiver through the inhomogeneous medium ..... 36
Figure 3.3	Illustration of medium structure in (a) Model I, (b) Model II and (c) Model III..... 37
Figure 3.4	Interaction of photon with the ith boundary extracted from (Vali et al., 2017)..... 39
Figure 3.5	The vertical profiles of attenuation coefficients based on chlorophyll concentration..... 42
Figure 3.6	The refractive index profiles calculated from empirical formula (Millard & Seaver, 1990) based on temperature, salinity, and pressure ..... 42
Figure 3.7	The line-of-sight of transmitter, Tx and receiver, Rx with description of beam divergence angle, FOV and aperture ..... 44



Figure 3.8	The effect of multiple scattering on the temporal dispersion of an impulse of light propagating in an underwater environment from (Cox Jr., 2012) .....	45
Figure 4.1	Normalised received power against the depth in low chlorophyll concentration for different models and sources .....	50
Figure 4.2	Normalised received power against the depth in high chlorophyll concentration for different models and sources .....	52
Figure 4.3	CIR of collimated link in low chlorophyll concentration at 5 m and 25 m of link range. ....	54
Figure 4.4	CIR of collimated link in high chlorophyll concentration at 5 m and 25 m of link range. ....	55
Figure 4.5	CIR of diffused link in low chlorophyll concentration at 5 m and 25 m of link range. ....	56
Figure 4.6	CIR of diffused link in high chlorophyll concentration at 5 m and 25 m of link range .....	57
Figure 4.7	FR of collimated link in low chlorophyll concentration at 5 m and 25 m of link range. ....	60
Figure 4.8	FR of collimated link in high chlorophyll concentration at 5 m and 25 m of link range. ....	61
Figure 4.9	FR of diffused link in low chlorophyll concentration at 5 m and 25 m of link range. ....	62
Figure 4.10	FR of diffused link in high chlorophyll concentration at 5 m and 25 m of link range. ....	63
Figure 4.11	The normalised received power against depth with 180°, 90°, 45°, 16° FOV and 4-inches aperture in low chlorophyll concentration water.....	66
Figure 4.12	The normalised received power against depth with 180°, 90°, 45°, 16° FOV and 4-inches aperture in high chlorophyll concentration water.....	67

Figure 4.13	The frequency responses of Model III for collimated source at low chlorophyll concentration water.....	69
Figure 4.14	The frequency responses of Model III for diffused source at low chlorophyll concentration water.....	70
Figure 4.15	The frequency responses of Model III for collimated source at high chlorophyll concentration water.....	71
Figure 4.16	The frequency responses of Model III for diffused source at high chlorophyll concentration water.....	72
Figure 4.17	The normalised received power against depth with 4, 3, 2, 1- inches aperture and 180° FOV in low chlorophyll concentration water.....	74
Figure 4.18	The normalised received power against depth with 4, 3, 2, 1- inches aperture and 180° FOV in high chlorophyll concentration water.....	75
Figure 4.19	Frequency response of Model III for collimated source at low chlorophyll concentration water.....	77
Figure 4.20	Frequency response of Model III for diffused source at low chlorophyll concentration water.....	78
Figure 4.21	Frequency response of Model III for collimated source at high chlorophyll concentration water.....	79
Figure 4.22	Frequency response of Model III for diffused source at high chlorophyll concentration water.....	80
Figure 4.23	Path loss and estimated bandwidth in water with low and high chlorophyll concentration against FOV for aperture size from 1 to 4-inches .....	84

## LIST OF SYMBOLS

$\lambda$	Wavelength of light
$\Phi$	Spectral radiant power
$\Phi$	Azimuthal angle
$\Theta$	Polar angle
$\mu$	Direction cosines

## LIST OF ABBREVIATIONS

BER	Bit-error-rate
FOV	Field-of-view
ISI	Inter-symbol interference
LED	Light emitting diode
LOS	Line-of-sight
MC	Monte Carlo
OWC	Optical wireless communication
OFDM	Orthogonal frequency division multiplexing
QAM	Quadrature amplitude modulation
RF	Radio frequency
RTE	Radiative transfer equation
UWC	Underwater wireless communication
UOWC	Underwater optical wireless communication
WBLD	White blue laser diode

## LIST OF APPENDICES

Appendix A      Table of computed PDF for Petzold's measurement

# **PEMODELAN PAUTAN MENEGAK TAK HOMOGEN KOMUNIKASI OPTIK TANPA WAYAR BAWAH AIR**

## **ABSTRAK**

Komunikasi wayarles optik bawah air (UOWC) menjadi semakin meluas, melangkaui sekatan sebelumnya kepada aplikasi ketenteraan dan pertahanan hingga kini turut digunakan dalam bidang komersial. Walaupun semakin popular, mereka bentuk sistem UOWC adalah mencabar kerana interaksi kompleks cahaya dengan air. Untuk mengatasi cabaran ini, tesis ini mencadangkan penggunaan medium tidak homogen dalam pemodelan saluran UOWC, berbanding model medium homogen tradisional yang menganggap nilai tetap tunggal untuk sifat fizikal dan kimia lautan. Tesis ini membentangkan dua model tidak homogen: Model II, berdasarkan variasi dalam kepekatan klorofil, dan Model III, yang merangkumi variasi dalam kedua-dua kepekatan klorofil dan indeks biasan. Model-model ini dibandingkan dengan Model I, model homogen. Untuk menganggarkan kuasa yang diterima, lebar jalur saluran dan penyebaran kelewatan, teknik Monte Carlo (MC) telah dipertingkatkan untuk mengambil kira ketidakhomogenan medium. Keputusan perbandingan menunjukkan peningkatan yang ketara dalam kuasa yang diterima, penurunan penyebaran kelewatan dan peningkatan lebar jalur untuk Model II dan III. Kesan ketidakhomogenan medium pada kedua-dua sumber cahaya selari dan tersebar serta ciri-ciri penerima juga dinilai. Secara keseluruhannya, model tidak homogen yang dicadangkan menunjukkan prestasi yang lebih baik berbanding model homogen tradisional, namun prestasi berkurangan diperhatikan dalam air dengan kepekatan klorofil yang tinggi disebabkan oleh keadaan persekitaran yang keruh. Walau bagaimanapun, Model II dan III belum lagi diuji atau disahkan secara meluas dan

memerlukan penyelidikan lanjut untuk menentukan kebolehpercayaan dan ketepatannya. Walaupun begitu, model ini boleh berguna sebagai alat rujukan untuk penyelidik lain meneroka kelakuan media tidak homogen dalam saluran penyebaran foton.

# **MODELLING OF INHOMOGENEOUS VERTICAL UNDERWATER OPTICAL WIRELESS COMMUNICATION LINKS**

## **ABSTRACT**

Underwater optical wireless communication (UOWC) is becoming increasingly widespread, moving beyond its former restriction to military and defense applications to now also being used in commercial fields. Despite its growing popularity, designing UOWC systems is challenging due to the complex interaction of light with water. To overcome these challenges, this thesis proposes using inhomogeneous medium in UOWC channel modeling, as opposed to the traditional homogeneous medium model which assumes a single constant value for the ocean's physical and chemical properties. The thesis presents two inhomogeneous models: Model II, based on the variation in chlorophyll concentration, and Model III, which includes the variation in both chlorophyll concentration and refractive index. These models are compared to Model I, the homogeneous model. To estimate the received power, channel bandwidth, and delay spread, the Monte Carlo (MC) technique was improved to account for medium inhomogeneity. The results of the comparison showed significant gains in received power, decreased delay spread, and increased bandwidth for Models II and III. The effect of medium inhomogeneity on both collimated and diffused sources and receiver parameters was also evaluated. Overall, the proposed inhomogeneous models showed improved performance compared to the traditional homogeneous model, with some deviations observed in water with high chlorophyll concentration due to severe environmental conditions. However, the Model II and III has not yet been extensively tested or validated and requires further research to determine its



reliability and accuracy. Despite this, the model could be useful as a reference tool for other researchers exploring the behavior of inhomogeneous media in photon propagation channels.

# CHAPTER 1

## INTRODUCTION

### 1.1 Introduction

The use of optical wireless communication (OWC) or free space optics (FSO) as a complementary technology to acoustics and radio frequency (RF) technologies in underwater wireless communications (UWC) has become a very promising area of research and development. Optical wireless carrier is a viable choice for low-latency, high bandwidth and high-data rate communication in the underwater environment because of radio frequency (RF) has a short propagation distance less than 10 m and acoustics carrier has a low data rate in kb/s (Islam et al., 2022). Specifically, laser or light-emitting diode (LED) sources are employed as the transmitter in underwater optical wireless communication (UOWC), depending on the application. Laser-based systems are preferred for power efficient and high data rate links (Jasman, 2016). But because a laser beam is collimated, this type of source still has a hard time maintaining accurate pointing and tracking, even though lasers can provide a high data rate. To solve these issues, a diffused source as LED is used.

Despite all of the benefits listed above, UOWC link suffer from substantial channel impairments due to the inherent optical characteristics (IOP) of seawater, namely absorption and scattering. Absorption and scattering are the inherent physical properties of water; they cause power loss and time dispersion [i.e., inter-symbol-interference (ISI)], resulting in poorer link performance such as high path loss and high delay spread and shorter transmission spans (to less than 100 m), as documented in multiple literatures (Ali et al., 2020; Gussen et al., 2016; Islam et al., 2022; Zhu et al., 2020). It is generally known that seawater has a low-loss property in blue and green lights (i.e., a transmission window of 450–550 nm) (Duntley, 1963; Zeng et al.,

2017), which has served as the foundation for future UOWC development. Thus, UOWC is seen as a complementary technology rather than alternative to the existing technology in underwater wireless communications. Figure 1.1 depicted the network of sensor and underwater vehicles comprised of submarine, autonomous underwater vehicle (AUV) and remotely operated vehicle (ROV) which utilizing multiple wireless carriers.

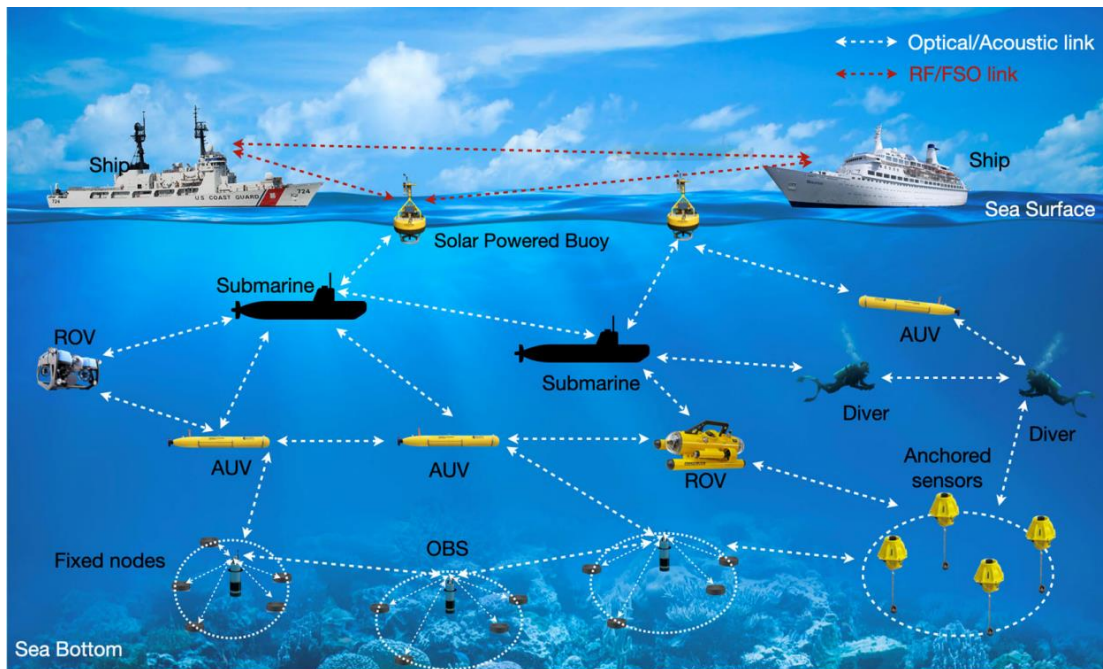


Figure 1.1 The basic structure of an underwater wireless communication adapted from (Wang et al., 2021)

Turbulence in the underwater environment is also a critical aspect of the problem of optical signal intensity loss, as it is caused by the fluctuation of refractive index due to variation of salinity and temperature (Elamassie & Uysal, 2020). This, in combination with absorption and scattering, contributes to the difficulty in predicting system performance for UOWC. Turbulence field testing is difficult, expensive, and time-consuming because of the irregular and unpredictable motions in oceans. Therefore, a basic simulation platform is required for predicting system performance prior to any system design, implementation, or evaluation. Despite

previous research has modelled and experimentally evaluated the absorption and multiple scattering processes (Cochenour, 2013; Jasman, 2016; Majlesein et al., 2018; M.G. Kraemer et al., 2020; Yuan et al., 2020), there are no combination of absorption, scattering and turbulence models of UOWCs using Monte Carlo (MC) simulation to our knowledge. Table 1.1 shows the description of UWC system that used three main wireless carriers.

Table 1.1 Description of UWC technologies from (Ali et al., 2020; Islam et al., 2022)

<b>Feature</b>	<b>RF waves</b>	<b>Acoustics waves</b>	<b>Optical waves</b>
<b>Range</b>	< 10 m	< 20 km	< 100 m
<b>Bandwidth</b>	30 – 300 Hz	10 – 1000 Hz	$10^{12} - 10^{15}$ Hz
<b>Data rate</b>	1–10 Mbps for 1–2 m 50–100 bps for 200 m	1.5–50 kbps for 0.5 km 0.6–3.0 kbps for 28–120 km	1 Gbps for 2m 1 Mbps for 25 m
<b>Affected factors</b>	Conductivity of channel permittivity of channel	of Pressure Temperature of Salinity of channel	of water Absorption Scattering Turbidity Organic matter of channel link

## 1.2 Problem statement and motivations

In a wireless communication system, the channel refers to the medium through which the information is transmitted from the transmitter to the receiver. This medium can be the air, water, or any other material, and the characteristics of the medium can significantly affect the transmission of the signal. In a wireless system that uses underwater optical communication (UWOC), the medium is water, which has unique characteristics that must be taken into account in the design of the system.

Channel modeling is the process of analyzing and modeling the characteristics of the channel in a communication system. In an UWOC system, this includes understanding how the water affects the transmission of light, how the

signal is attenuated as it travels through the water, and how the signal is affected by the movement of the water and other factors such as temperature and pressure.

By understanding the characteristics of the channel, engineers can design systems that are better able to transmit information over long distances and in challenging conditions. This can help to improve the performance of the system and increase its reliability.

In this work, the effect of seawater vertical properties (i.e., depth-dependent chlorophyll concentration and refractive index) on UOWC performance has not been emphasized in recent channel model studies.

According to recent studies done by Xu et. al., 2022, the channel model developed uses the assumption that the water medium is homogeneous. They used a constant value of the attenuation coefficient  $c$  to describe a homogeneous water medium, their assumption still applies to open water. The model needed now is one that uses an inhomogeneous water medium to describe the behavior of light in water whose properties change at every depth. Recent study done by Kumar et. al., 2021 attempt to develop such channel model with combined absorption, scattering, and turbulence but unfortunately the study disregards the variation of attenuation coefficient due to depth. In order to fill the gaps, the model developed in this thesis is one that considered the three effects of variation of absorption, scattering and turbulence with depth in the channel model to predict the correct behavior of light in water.

Additionally, Anous et. al., 2018 stated that UOWC experiments are expensive and difficult to implement in real time due to the complex nature of seawater. By developing a realistic channel model that considers all three effects it is useful to be a reference model and to design a reliable UOWC system. A model that

mimics the behavior of photons with a real underwater environment will make it easier and faster for designers to predict the effect on channel characteristics (impulse response and frequency) using different receiver parameters. Information about these channel characteristics will allow designers to make better decisions before implementing the system in real conditions.

This model can be used to select optimal receiver parameters (aperture size and receiver FOV) based on predicted power and bandwidth performance at different channel conditions (chlorophyll concentration and light source type). For example, a model from Cox Jr, 2012 named Photonator is useful for predicting optimal receiver parameters for line-of-sight underwater communication links using laser or LED in high turbidity water (high chlorophyll concentration water and high turbidity). This model can help solve the difficulty of developing and testing receiver design in an underwater environment to obtain operational data.

In brief, this thesis's goals are to develop a channel model with vertical properties of underwater, analyse the effect of different receiver parameter on channel characteristics and propose optimal design of receiver parameter on various channel conditions.

### **1.3 Objectives**

The aim of this thesis is to have a realistic channel model by considering the effect of inhomogeneous medium associated with vertical link. As stated before, there are many channel models of underwater optical wireless communication that assume ocean water as a homogeneous medium. Therefore, the objectives of this work are listed as follows:

-To develop channel model that incorporates the vertical properties of ocean water

-To evaluate the effect of different receiver parameters on the channel characteristics

-To propose the optimum design of receiver parameters for different channel conditions

#### **1.4 Scope of research**

The scope of the study is focused on channel modelling with MC method to describe light propagation in vertical depth of underwater environment for a line-of-sight (LOS) link between transmitter and receiver using MATLAB software. The LOS link is chosen because it is a simple scenario and does not complicate the simulation in studying the effects of medium inhomogeneity. The simulation will be using different receiver parameters such as field-of-view (FOV) and aperture to analyse the link performance which consists of path loss, impulse and frequency responses. This is done to allow researchers to study the effects of receiver parameters under a variety of different conditions and scenarios, which can be useful for understanding how the UWOC system will perform in real-world environments. Additionally, this simulation also helpful to system designer to optimize the design of the UWOC system by identifying which receiver parameters have the greatest impact on performance and how they should be adjusted in order to maximize the effectiveness of the system.

## 1.5 Thesis outline

The rest of this thesis is structured as follows: Chapter 2 provides a thorough review of UWC literature in terms of history, characteristics, advantages, and disadvantages of various types of wireless carriers (e.g., acoustics, RF, and optical waves). This section also includes an introduction to the physical properties of the ocean that affect light propagation in underwater, including a discussion of absorption, scattering, and turbulence caused by refractive index fluctuation. In addition, an introduction to the radiative transfer equation, which governs the complex behaviour of light in under water, is discussed in this section radiative transfer equation (RTE). In addition, the most commonly used channel model, Beer-Lambert law, is compared to RTE and its limitations.

Chapter 3 introduces numerical techniques and the mechanics of light propagation underwater. The theory and principle underlying the MC techniques used to numerically solve RTE are described, along with its mathematical equation. The distinction between homogeneous (i.e., Model I) and inhomogeneous (i.e., Model II and III) channel models is also thoroughly explained, as is how different layers of the ocean affect light propagation. This section also contains all of the simulation parameters used to model collimated and diffused sources, also known as laser and LED.

In addition, in Chapter 4, the simulation result is prepared by analysing the channel characteristics, such as path loss, impulse response, and frequency response. This section also discusses the effect of the receiver's aperture and field-of-view (FOV) on channel characteristics, as well as design considerations for a reliable UOWC system. Lastly, chapter 5 summarizes the thesis's contributions and emphasises several recommendations for future work.



## **CHAPTER 2**

### **LITERATURE REVIEW**

#### **2.1 Introduction**

The purpose of this literature review is to provide the reader with a general overview of underwater wireless communication and underwater optical properties used in the channel modelling. Underwater wireless communications (UWC) have always been an important asset in decades for the marine research, oceanography, offshore industry and military development. The first part of this chapter gives a brief description of underwater wireless communication and its advantages and limitations. Next, an overview of underwater optical wireless communication is presented. The optical properties associated with underwater environment is addressed to explain the complexity interaction of light with ocean water. Furthermore, the depth-dependent optical properties and the associated numerical methods (e.g., Beer's law and radiative transfer equation) are reviewed in order to describe light-water interaction. Lastly, the summary of recent work on channel modelling is presented.

#### **2.2 Overview on underwater wireless communication**

Underwater wireless communications (UWC) are critical in a variety of maritime operations, including environmental monitoring, underwater exploration, and the collecting of scientific data. The peculiar and severe circumstances that define underwater channels, make underwater wireless communications to be a difficult endeavour. These circumstances include, for example, significant attenuation, multipath dispersion, and a restricted ability to use available bandwidth

of the signals. Currently, there are three types of UWC: underwater acoustic communication (UAC), underwater radio frequency (RF) communication and underwater optical wireless communication (UOWC). Acoustic waves are the most effective means of communicating underwater, and the first practical underwater acoustic communication (UAC) device was an underwater telephone, which was created in 1945 in the United States for communication with submarines. It employed a single side-band suppressed carrier modulation in the 8-11 kHz range, and it was capable of operating over a distance of several kilometres. However, there are a number of factors that influence the propagation of acoustic waves under water. Refraction and reflection cause acoustic waves to bend and refract as they pass through water. There are a number of factors that influence the reflection and refraction of acoustic waves, including water temperature, depth, salinity, and shadowing zones. Refraction and reflection cause acoustic waves travelling over water to experience multipath propagation and fading. These phenomena severely limit performance, resulting in data rates of only a few kbps, bandwidths of 10 kHz, and propagation delays of 0.67 s/km (Zhu et al., 2020).

Meanwhile, RF communication has a smoother transition through the air/water interface than UAC and is more tolerant of water turbulence (Che et al., 2010). The transmission of RF signals at 10 kHz and 10 MHz in sea water is 100 to 2000 times faster than acoustic, resulting in an advantaged command latency (Che et al., 2010). Only ultra-low frequencies between 30 and 300 Hz may propagate through conductive salty water due to the signal attenuation happening at the higher frequencies (Kaushal & Kaddoum, 2016). A restricted data rate of a few Mbps can be achieved by using low modulation bandwidth RF transmission at a short range up to 10 m (Kaushal & Kaddoum, 2016).

As an alternative, underwater optical wireless communication (UOWC) is a method to overcome the shortcomings of underwater RF communication and UAC such as excessive power consumption, latency, and incompatibility of high speed and long distance. The following section discusses UOWC in more details.

### 2.3 Underwater optical wireless communication

Underwater optical wireless communication is a form of optical communication in which visible or ultraviolet (UV) light is used to carry a signal in underwater environment. UOWC transmission is accomplished by modulating data with a light source, typically an LED or laser, and detecting it with a photodetector. Signal processing and demodulation occur on the receiver part in order to retrieve the original data. Figure 2.1 shows an example of underwater optical communication in block diagram.

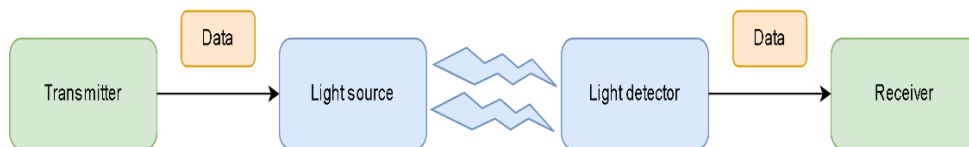


Figure 2.1 Illustration of underwater optical wireless communication

UOWC systems are very similar to visible light communication (VLC) systems, which utilise laser diodes (LDs) and light-emitting-diodes (LEDs) as potential light sources. The visible light spectrum (400–700 nm) of LD or LED used in UOWC systems is modulated in various modulation techniques in order to efficiently transfer data. Both light sources are quite interesting; LDs because of their larger modulation bandwidth when compared to LEDs, although the latter, because of their higher power efficiency, lower cost, and longer lifetime, appear to be more suitable for medium bit rate applications than the former. The invention of LDs and

LEDs in 1962 by (Hall et al., 1962) and (Holonyak & Bevacqua, 1962) have propelled the development of UOWC system. Currently, the LDs' capabilities of large modulation bandwidth of hundreds of MHz (Kaushal & Kaddoum, 2016) or perhaps GHz (Lee et al., 2015) allows it to achieve data rates exceeding Gbps. It is also possible to transmit data over distances of hundreds of metres (Zhu et al., 2020). Moreover, with a low transmission latency of 100 ms (Zhu et al., 2020), these high-speed and long-distance benefits of LDs will allow various real-time applications such as underwater digital video streaming and untethered remotely operated vehicle (UTROV) among others. The LDs require a sophisticated pointing and alignment system before being able to transmit long distance due to the narrow beam and small divergence. On the other hands, LEDs are a viable candidate due to the advantages of its large light beam, compact structure, low cost, and low power consumption.

Similar to other underwater wireless communication systems, namely UAC and RF, UOWC is greatly affected by the transmission medium. Duntley proposed in 1963 that light with a wavelength between 450 and 550 nm had less attenuation caused by underwater absorption and scattering (Duntley, 1963). This study established the existence of a need for using only blue-green light spectrum in underwater communications, and furthermore laid the groundwork for the future development of UOWC. Figure 2.2 below illustrates the absorption coefficient of light in pure seawater.

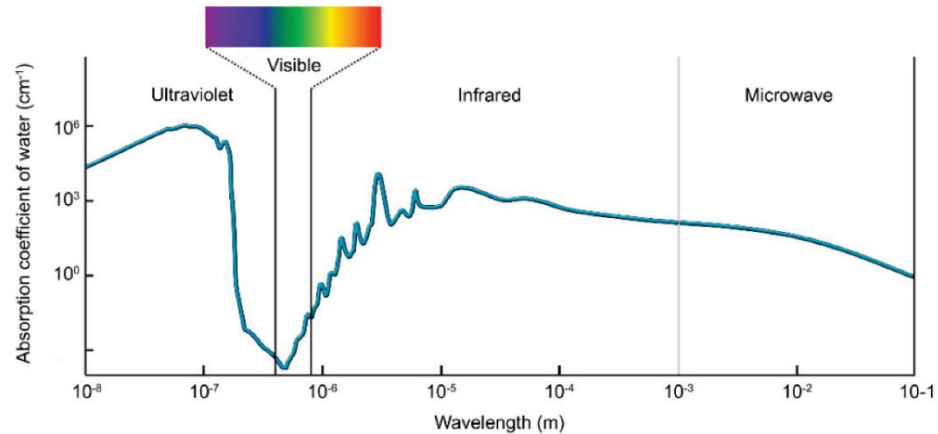


Figure 2.2 Absorption coefficient of pure seawater for different light wavelengths extracted from (Schirripa Spagnolo et al., 2020)

The environment of coastal waters and oceanic waters are challenging to the UOWC system due to the complexity of light propagation, therefore making experiments and performance evaluation of the system difficult to design and implement. There are two distinct optical properties of water: inherent optical properties (IOP) and apparent optical properties (AOP) (Mobley, 1994). IOP are optical characteristics composed mostly of the absorption and scattering coefficients that are completely dependent on the transmission medium used to measure them. Meanwhile, AOP are related to the geometric structure of the light source and transmission medium. In comparison to AOP, IOP have a greater impact on UOWC performance, and most research focuses on IOP in UOWC. This topic on IOP is further explained in Section 2.4. IOP is normally considered as a constant value (Johnson et al., 2013) (Anous et al., 2018) (Sahoo et al., 2019). The ocean's nature is depth-dependent, resulting in variations in underwater optical properties, which will be discussed in greater detail in Section 2.5.

## 2.4 Inherent optical properties

One of two things can happen when light interacts with matter. Light's energy can be transferred to another form, such as heat or the energy contained in a chemical bond, causing it to vanish. This is referred to as absorption. Light can also change its wavelength and/or direction. Either of these processes is referred to as scattering. The inherent optical properties, or IOPs, of a medium, such as sea water, describe its absorption and scattering properties. Figure 2.3 illustrates the geometry used to describe the concept of the inherent optical properties of water.

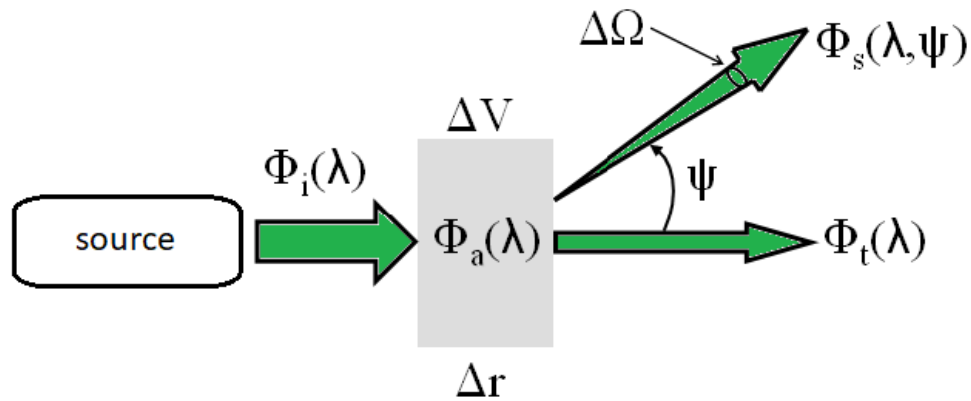


Figure 2.3 Geometry used to define the inherent optical properties of water from (Mobley 1994)

A beam of monochromatic light of spectral radiant power at wavelength  $\lambda$ ,  $\Phi_i(\lambda)$  in  $\text{W nm}^{-1}$ , illuminates a volume of water  $\Delta V$  with thickness  $\Delta r$ , as depicted in Figure 2.1. A quantity of the radiant power is absorbed,  $\Phi_a(\lambda)$  and scattered at an angle  $\psi$ ,  $\Phi_s(\lambda, \psi)$  within the volume of water. The rest of the beam's power,  $\Phi_t(\lambda)$  transmits through the volume with no change in direction. Assuming that the light does not undergo a change in wavelength during the scattering process and the whole processes follow the conservation of energy, then

$$\Phi_i(\lambda) = \Phi_a(\lambda) + \Phi_s(\lambda) + \Phi_t(\lambda) \quad (2.1)$$

where  $\Phi_s(\lambda)$  is the total power that is scattered into all directions. The absorptance  $A(\lambda)$ , scatterance  $B(\lambda)$ , and transmittance  $T(\lambda)$  are respectively the fractions of incident power that are absorbed, scattered, and transmitted within the volume, such as

$$A(\lambda) = \frac{\Phi_a(\lambda)}{\Phi_i(\lambda)} \quad (2.2)$$

$$B(\lambda) = \frac{\Phi_s(\lambda)}{\Phi_i(\lambda)} \quad (2.3)$$

$$T(\lambda) = \frac{\Phi_t(\lambda)}{\Phi_i(\lambda)} \quad (2.4)$$

These quantities are then divided by the thickness  $\Delta r$ , as it approaches zero, to obtain the absorption  $a(\lambda)$  and scattering  $b(\lambda)$  coefficients which are respectively the inherent optical properties.

$$a(\lambda) = \lim_{\Delta r \rightarrow 0} \frac{\Delta A(\lambda)}{\Delta r} = \frac{dA(\lambda)}{dr} \quad (2.5)$$

$$b(\lambda) = \lim_{\Delta r \rightarrow 0} \frac{\Delta B(\lambda)}{\Delta r} = \frac{dB(\lambda)}{dr} \quad (2.6)$$

Additionally, the total of these coefficients is defined as the attenuation coefficient  $c(\lambda)$ .

$$c(\lambda) = a(\lambda) + b(\lambda) \quad (2.7)$$

where all of these coefficients are in units of  $m^{-1}$ . Another IOP that is commonly used is the single-scattering albedo  $\omega(\lambda)$

$$\omega(\lambda) = \frac{b(\lambda)}{c(\lambda)} \quad (2.8)$$

where  $\omega(\lambda)$  in unit of  $m^{-1}$  is the probability that a photon will be scattered (rather than absorbed) in any given interaction between photon and matter, which will be described in the next chapter.

#### 2.4.1 Absorption and scattering coefficients

Many works describe attenuation coefficient,  $c(\lambda)$  as a single value at a specific wavelength, neglecting the variations of  $a(\lambda)$  and  $b(\lambda)$  with depth. This assumption is only applicable for the open oceans, where scattering is minimal (Anous et al., 2018). The absorption coefficient  $a$  in Equation (2.7) is actually an addition of absorption spectra multiplied by their respective concentrations, such that

$$a(\lambda) = a_w(\lambda) + a_f^0 C_f \exp(-k_f \lambda) + a_h^0 C_h \exp(-k_h \lambda) + a_c^0(\lambda)(C_c(z))^{0.602} \quad (2.9)$$

where  $a_w$  is pure water absorption coefficient in  $m^{-1}$ ;  $a_f^0$  is specific absorption coefficient of fulvic;  $a_h^0$  is specific absorption coefficient of humic acid;  $a_c^0$  is specific absorption coefficient of chlorophyll in  $m^{-1}$ ;  $C_f$  is the concentration of fulvic acid in  $mg/m^3$ ;  $C_h$  is the concentration of humic acid in  $mg/m^3$ ;  $C_c$  is the vertical distribution of concentration of chlorophyll-a in  $mg/m^3$ ;  $k_f$  is the fulvic acid exponential coefficient and  $k_h$  is the humic acid exponential coefficient. Moreover, the scattering coefficient  $b$  in Equation (2.7) is mainly influenced by two biological factors, scattered by pure water and particulate matter which is characterized as

$$b(\lambda) = b_w(\lambda) + b_s^0(\lambda) C_s + b_l^0(\lambda) C_l \quad (2.10)$$

where  $b_w$  is the pure water scattering coefficient in  $m^{-1}$ ;  $b_s^0$  is the scattering coefficient for small particulate matter in  $m^2/g$ ;  $b_l^0$  is the scattering coefficient for large particulate matter in  $m^2/g$ ;  $C_s$  is the concentration of small particles in  $g/m^3$  and



$C_l$  is the concentration of large particles in  $\text{mg/m}^3$ . Equation 2.9 and 2.10 can be found further in detail in (Johnson et al., 2013).

#### 2.4.2 Volume scattering function

Scattering occurs when an optical beam is deflected from its original path due to suspended particles or a change in the density or refractive index of the medium, resulting in reflection or refraction. For modelling the scattering of light by suspended particles, a volume scattering function (VSF),  $\beta(\theta, \lambda)$  is defined as the ratio of the scattered light's angular distribution to the incident irradiance per unit volume. When incident light is not polarized and the water is isotropic, scattering becomes angular-dependent. It is defined as the fraction of scattered power that passes through an angle and becomes a solid angle and the associated VSF is denoted by

$$\beta(\theta, \lambda) = \lim_{\Delta r \rightarrow 0} \lim_{\Delta \Omega \rightarrow 0} \frac{\Delta \beta(\theta, \lambda)}{\Delta r \Delta \Omega} \quad (2.11)$$

The total scattered power per unit irradiance, or scattering coefficient,  $b(\lambda)$ , is calculated by integrating  $\beta(\theta, \lambda)$  over all angles in the manner described below

$$b(\lambda) = 2\pi \int_0^\pi \beta(\theta, \lambda) \sin \theta \, d\theta \quad (2.12)$$

The scattering phase function (SPF) is defined as the angular distribution of light intensity scattered by a particle at a given wavelength such as

$$\tilde{\beta} = \frac{\beta(\theta, \lambda)}{b(\lambda)} \quad (2.13)$$

SPF is typically represented as the Henyey-Greenstein (HG) function, which was originally proposed for galactic scattering (Henyey & Greenstein, 1941) and often used in a modified form (Ertürk & Howell, 2017) as

$$\tilde{\beta} = P_{HG}(\theta, \lambda) = \frac{1-g^2}{4\pi(1+g^2-2g\cos\theta)^{3/2}} \quad (2.14)$$

where  $g$  denotes the HG asymmetry parameter, which is medium-dependent and equal to the average cosine of the scattering angle  $\cos\theta$  in all scattering directions. However, HG function fails to provide adequate results for light scattering with small ( $\theta < 20^\circ$ ) and large ( $\theta > 130^\circ$ ) angles (Li et al., 2018). Therefore, the simulation will instead use the VSF based on the Petzold scattering measurement (Petzold, 1972) which can be readily accessed in tabulated form as in Appendix A. Petzold measurement can provide detailed information about the size, shape, and distribution of the scatterers within the water, as well as the anisotropy of the scattering, which can be important for accurately modeling the transmission of light in different directions in the underwater environment (M.G. Kraemer et al., 2020). Using this measurement to describe the scattering function in an underwater optical wireless communication simulation can be beneficial because it provides a direct measurement of the scattering properties of the water, which can be important for accurately modeling the optical transmission in the underwater environment.

## 2.5 Vertical link properties

As mentioned previously in Section 2.3, the ocean environment changes with vertical depth, resulting in changes in underwater optical properties as well. The optical properties of water are dependent on several parameters such as salinity, temperature, and pressure (Anous et al., 2018). Water pressure in vertical links increases by 10 dbar for every 10 m of depth, while temperature decreases significantly from  $25^\circ\text{C}$  to almost  $0^\circ\text{C}$  (Anous et al., 2018). The salinity of water varies with depth and has a direct effect on the refractive index of water. These depth

dependent parameters emphasise the importance of considering the impact of such inhomogeneous underwater environment models on the UOWC system.

### 2.5.1 Vertical distribution of chlorophyll-a

Chlorophyll-a is the major component of phytoplankton, a category of tiny organisms. They only live in the photic or euphotic zone, which is the region of the ocean where sunlight may propagate. Another requirement for photosynthesis is nutrient availability, which is often higher in coastal locations due to surface runoff from land and subsurface water upwelling into the photic zone. The chlorophyll profile over a depth  $z$  from the surface can be modelled as a Gaussian curve that include five parameters numerically computed (Kameda & Matsumura, 1998)

$$C_c(z) = B_0 + Sz + \frac{h}{\sigma\sqrt{2\pi}} e^{-\frac{(z-z_{\max})^2}{2\sigma^2}} \quad (2.15.1)$$

$$\sigma = \frac{h}{[\sqrt{2\pi}(C_{z_{\max}} - B_0 - Sz_{\max})]} \quad (2.15.2)$$

where  $C_c(z)$  is the chlorophyll concentration ( $\text{mg}/\text{m}^3$ ) at depth  $z$  (m),  $B_0$  is the background chlorophyll concentration at sea surface ( $\text{mg}/\text{m}^3$ ),  $S$  is the vertical gradient of the chlorophyll concentration ( $\text{mg}/\text{m}^3/\text{m}$ ),  $h$  is the total chlorophyll above the background ( $\text{mg}/\text{m}^2$ ),  $\sigma$ , standard deviation of Gaussian distribution, controls the thickness of the chlorophyll maximum layer (m), and  $z_{\max}$  is the depth of the chlorophyll maximum (m).

### 2.5.2 Depth dependent refractive index

Oceanic turbulence is caused by the variations of the refractive index,  $n$  of the water, which fluctuates the received light intensity. In the model for vertical profile of refractive index proposed by (Millard & Seaver, 1990), the variation of  $n$  is based upon the composition of the water, i.e., water pressure  $P$ , wavelength  $\lambda$ , temperature

$T$ , and salinity  $S$  and the model is valid for  $500 < \lambda < 700$  nm,  $0 < T < 30^\circ\text{C}$ ,  $0 < S < 40$  psu, and  $0 < P < 11000$  dbar.

$$\begin{aligned}
n(T, P, S, \lambda) = & n_0 + n_1\lambda^2 + n_2\lambda^{-2} + n_3\lambda^{-4} + n_4\lambda^{-6} + n_5T + n_6T^2 + n_7T^3 + \\
& n_8T^4 + (n_9T + n_{10}T^2 + n_{11}T^3)\lambda + (n_{12} + n_{13}\lambda^{-2} + n_{14}T + n_{15}T^2 + \\
& n_{16}T^3)S + n_{17}ST\lambda + n_{18}P + n_{19}P^2 + n_{20}P\lambda^{-2} + (n_{21}T + n_{22}T^2)P + \\
& n_{23}P^2T^2 + (n_{24} + n_{25}T + n_{26}T^2)PS
\end{aligned} \tag{2.16}$$

The coefficients in Equation (2.16) can be found in detail in (Anous et al., 2018) and (Millard & Seaver, 1990). The values of  $T$  and  $S$  are adapted from (Castelão, 2017) which provides a climatologic data on any requested coordinates.

## 2.6 Beer's law and radiative transfer equation

There are two common methods that can be used to model UOWC link, namely Beer-Lambert law and radiative transfer equation (RTE) (Wang et al., 2021). Beer-Lambert law uses attenuation coefficient to describe the loss of light over a path length,  $z$ . Assuming the differential path loss is

$$\frac{dI}{dr} = -cI \tag{2.17}$$

where  $I$  is the power intensity on the volume of width  $dr$ , and  $c$  is the attenuation coefficient as described in Equation (2.7). The negative  $c$  is to describe the light is lost over the path. Integrating Equation (2.17) yields

$$\int_{I_0}^I \frac{1}{I} dI = -c \int_0^r dr \tag{2.18}$$

$$\ln(I) - \ln(I_0) = -cr \tag{2.19}$$

which when simplified, yields the Beers Law expression, where  $I_0$  is the initial power intensity

$$I = I_0 e^{-cr} \quad (2.20)$$

The model is applicable for simple underwater environment where there is only absorption and no multiple scattering effects. To compensate the non-multiple scattering effect, the RTE is used to more accurately describe the light attenuation in the underwater environment by using the principle of energy conservation. The radiance of the beam is expressed as

$$L(z, \lambda, \phi, \theta) = \frac{P(z, \lambda, \phi, \theta)}{\Delta A \Delta \Omega \Delta \lambda} \quad (2.21)$$

where  $\Delta A$  is the area of the receiver,  $\Delta \Omega$  is the solid angle in the direction of  $\phi, \theta$ , and  $z$  is the link depth or the distance between transmitter and receiver in the ocean. Applying the radiance, the RTE for a simple homogeneous medium, with no internal sources like sunlight or bioluminescence and no inelastic scattering, is

$$\cos \theta \frac{dL(z, \lambda, \phi, \theta)}{dz} = -c(z, \lambda)L(z, \lambda, \phi, \theta) + \int_{4\pi} \beta(z, \lambda, \phi' \rightarrow \phi, \theta' \rightarrow \theta) L(z, \lambda, \phi', \theta') d\Omega' \quad (2.22)$$

where  $L(z, \lambda, \phi, \theta)$  represents the radiance at depth  $z$  in the direction  $\theta, \phi$ , the first term is the Beer's law, and the second term represents the gain from the light scattering from angle  $\theta', \phi'$  into direction  $\theta, \phi$ . The simplest case of RTE is difficult to solve (Yahia et al., 2021; Zhu et al., 2020), therefore MC technique is used to present a way to solve the equation in the next subsection.

## 2.7 Homogeneous model

This section presents the MC method that commonly used to describe photon propagation through a homogeneous underwater medium. In homogeneous medium,

the attenuation coefficient and the index of refraction are assumed to be constant. The Photonator (Cox Jr., 2012), a program written in the MATLAB language, represents an appropriate starting point in the search for existing modelling tools. The program has been shown to match experimental data in the laboratory for light attenuation from scattering and absorption under water due to Maalox acid. In this program, light is specifically modelled as a group of virtual photons or packets of photons and each photon is identified according to its position, direction and weight. Furthermore, the entire program uses a horizontal configuration to simulate photon propagation underwater. This Photonator program is modified in the photon geometric path length section and also the medium structure which is discussed further in Section 3.4.

### **2.7.1 Initial preparations**

The type of water environment, light sources, and receivers are determined first before launching the photon. The initial position and direction cosines of photons were also determined, and these involved the modelling of the polar and azimuthal angles of the sources (laser and LED). The receiver plane is positioned on the  $x$ - $y$  plane at a fixed location along the  $z$ -axis in the simulation geometry, which employed a Cartesian coordinate system as illustrated in Figure 3.1.

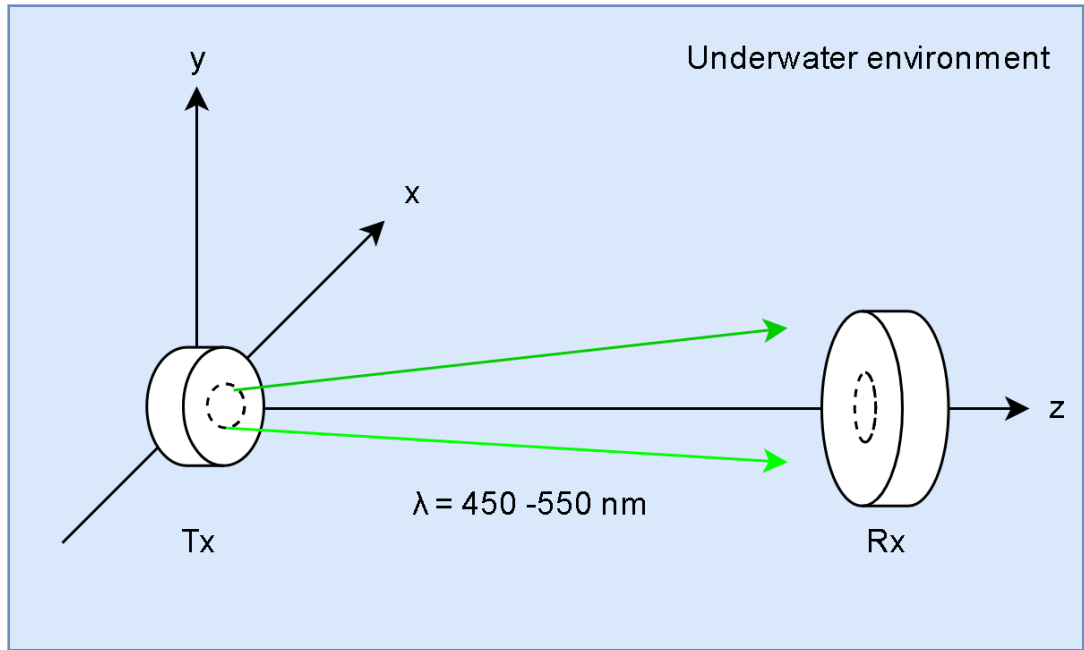


Figure 2.4 Transmitter (Tx) and receiver (Rx) in a Cartesian coordinate system with the appropriate wavelength for the underwater environment.

### 2.7.2 Initial photon position

Gaussian source distribution is the basis for modelling the radiation pattern of a laser beam and also can be an approximation to a LED beam. Consider a Gaussian laser beam profile of relative irradiance  $E(r)$ , where  $k$  is the  $1/e$  radius,

$$E(r) = \frac{e^{-r^2/k^2}}{\pi k^2} \quad (3.1)$$

The probability density function (PDF) describing the beam profile as a function of radial position  $r$  is

$$p(r) = \frac{e^{-r^2/k^2}}{\pi k^2} 2\pi r = \frac{e^{-r^2/k^2}}{k^2} 2r, \text{ where } \int_0^\infty p(r) dr = 1 \quad (3.2)$$

The cumulative distribution function (CDF)  $P(r)$  is obtained by integrating  $p(r)$

$$P(r) = \int_0^r p(r') dr' = 1 - e^{-r^2/k^2} \quad (3.3)$$

Equating the CDF with  $q$  and solving for initial radius,  $r$  yields

$$r = k\sqrt{-\ln(1-q)} \quad (3.4)$$

The modelled laser beam has a narrow divergence; therefore, a divergence lens is used to diverge the beam. The focal length  $f$  of the lens that diverge the beam is based on the equation

$$f = -\frac{b}{\phi_{div}} \quad (3.5)$$

where  $b$  is the beam waist and  $\phi_{div}$  is the half angle divergence. By using the equation 3.4 the polar angle  $\theta_0$  can be defined as

$$\theta_0 = -\frac{r}{f} \quad (3.6)$$

For the azimuthal angle  $\Phi_0$ , the values are chosen randomly on the uniform distribution of  $[0, 2\pi]$ . Then, the initial photon position is

$$x_0 = r \cos \Phi_0 \quad (3.7)$$

$$y_0 = r \sin \Phi_0 \quad (3.8)$$

and the initial direction cosines are defined by

$$\begin{bmatrix} \mu_x \\ \mu_y \\ \mu_z \end{bmatrix} = \begin{bmatrix} \sin \theta_0 \cos \Phi_0 \\ \sin \theta_0 \sin \Phi_0 \\ \cos \theta_0 \end{bmatrix} \quad (3.9)$$

### 2.7.3 Photon path length

The photon path length is defined as

$$l = cs \quad (3.10)$$

where  $c$  is the attenuation coefficient and  $s$  is the geometric distance between optical events. The PDF for the attenuation of light with respect to optical distance travelled  $p(l)$  is



$$p(l) = e^{-l}, l \geq 0 \quad (3.11)$$

The CDF  $P(l)$  is

$$P(l) = \int_0^l e^{-l'} dl' = 1 - e^{-l} \quad (3.12)$$

The CDF  $P(l)$  is then equated with  $q$  to determine  $l$

$$l = -\ln(1 - q) = -\ln(q), 0 \leq q \leq 1 \quad (3.13)$$

In homogeneous medium, the photon geometric path length  $s$  (in meters) can be calculated with (Leathers et al., 2004)

$$s = \frac{l}{c} = -\frac{\ln(q)}{c} \quad (3.14)$$

#### 2.7.4 Photon weight

After determining the path length, the weight and scattering direction of the photons were examined. The weight of photon is updated by multiplying with the scattering albedo  $\omega$ , given as

$$W_{n+1} = W_n \omega = W_n b/c \quad (3.15)$$

If the photon weight  $W_{n+1}$  falls below the predefined threshold, then the photon is terminated or boosted by the roulette such as

$$W_{n+1} = \begin{cases} mW_{n+1}, & \xi \leq 1/m \\ 0, & x > 1/m \end{cases} \quad (3.16)$$

where  $m$  is the roulette constant. When the photon survives the rouletting process, the new scattered direction must be updated using the angles computed from the scattering phase function as explained further in Section 3.3.6.